Anal. Chem. **2002,** *74,* 5364−5369

Miniaturized Flow Fractionation Device Assisted by a Pulsed Electric Field for Nanoparticle Separation

Alex I. K. Lao,[†] Dieter Trau,[‡] and I-Ming Hsing*,[†]

Department of Chemical Engineering, Bioengineering Graduate Program, Hong Kong University of Science and Technology, Clear Water Bay, Kowloon, Hong Kong

Electric field flow fractionation (EFFF) is a powerful separation technique based on an electrical field perpendicular to a pressure-driven flow. Previous studies of microelectric field flow fractionation (*μ*-EFFF) indicate that separation performance was limited due to a weak effective electric field caused by polarization layers on the electrode surfaces. In this work, we report on a *μ*-EFFF device that uses a pulsed voltage scheme to overcome these limitations. The device was fabricated in indium tin oxide (ITO)-coated glass with ITO as electrodes. The effective electric field for pulsed voltage operation was found to be 50-fold stronger when compared with constant voltage operation. A strong influence of pulsed voltage frequency on nanoparticle retention times was observed. Using pulsed voltage, improved separation of polystyrene particles of different surface charge and particle size is demonstrated. Pulsed voltage also offers more parameters compared to the constant voltage mode, e.g., pulse frequency, duty cycle, and waveform to optimize the retention behavior of analytes.

Micro total analysis systems (*μ*-TAS) have been a topic of growing interest over the past decades. They offer many advantages over conventional analysis tools including reduced analysis times, reduced sample/reagent volumes, increased parallelism, and portability. A *μ*-TAS capable of "sample in/answer out" operation requires multiple functions, e.g., sample preparation, separation, amplification, and detection. It is expected that *μ*-TAS will find widespread application in bioanalytics. Miniaturized devices for DNA amplification[1,2] and electrophoretic separation[3] have been successfully demonstrated. However, the technologies for sample preparation and separation in the microscale are still to be developed.

Microscale sample separation methods, which include filtration, dialysis, extraction, chromatography, and free-flow electrophoresis, are essential to build up a *μ*-TAS. Separation of leukocytes from blood was demonstrated by filtration.[4] However, this device suffered from clogging and membrane breakage. Chromatography has been successfully demonstrated in applications for DNA and proteins separations.[5] Biosample separation has been accomplished by free-flow electrophoresis.[6] But a complex microstructure acting as a fraction collector was needed to collect separated analytes simultaneously.

Electric Field Flow Fractionation (EFFF) as an Alternative Method to Achieve Sample Preparation in *μ*-TAS. The method is capable of separating biomolecules and particles over a broad size range. Protein separation by using EFFF was first demonstrated in 1972.[7] A poor separation performance was reported for this macroscale system, and little effort has been directed toward its improvement. In 1993, an improved design with channel walls built by electrodes was introduced.[8] Separation of latex particles and carbohydrates was successfully demonstrated in other similar systems.[9,10] EFFF gains numerous advantages from miniaturization, such as increased resolution, reduced analysis time, increased parallelism of analysis, and reduced system size.[10] The first micro-EFFF (*μ*-EFFF) system was introduced in 1997 for the separation of latex particles.[11] However, the effective potential across the EFFF channel is typically only a small fraction of the nominally applied voltage.[12,13] The bulk of the liquid in the channel is shielded from the electrodes by polarization layers of ions and water molecules on the electrode surfaces. Most of the potential drops at these electrical double layers leaving only a weak electric field in the channel effective for separation.

* Corresponding author. Fax: 852-2358-0054. E-mail: kehsing@ust.hk.
[†] Department of Chemical Engineering.
[‡] Bioengineering Graduate Program.

(1) Northrup, M. A.; Ching, M. T.; White, R. M.; Watspn, R. T. *Proc. 1993 IEEE Int. Conf. Solid-State Sens. Actuators* **1993**, 924−926.
(2) Lee, T. M. H.; Hsing, I. M.; Lao, A. I. K.; Carles, M. C. *Anal. Chem.* **2000**, *72*, 4242−4247.
(3) Fu, L. M.; Yang, R. J.; Lee, G. B. *Electrophoresis* **2002**, *23*, 602−612.
(4) Rijn, C. V.; Nijdam, W.; Elwenspoek, M. *Proc. 1996 18th Annual International Conference of IEEE Engineering in Medicine and Biology Society*, 1996; pp 256−257.
(5) Ericson, C.; Holm, J.; Ericson, T.; Hjerten, S. *Anal. Chem.* **2000**, *72*, 81−87.
(6) Raymond, D. E.; Manz, A.; Widmer, H. M. *Anal. Chem.* **1996**, *68*, 2515−2522.
(7) Caldwell, K. D.; Kesner, L. F.; Myer, M. N.; Giddings, J. C. *Science* **1972**, *176*, 296−298.
(8) Caldwell, K. D.; Gao, Y. S. *Anal. Chem.* **1993**, *65*, 1764−1772.
(9) Mori, R.; Nakagama, T.; Hobo, T. *Chromatography* **1994**, *15* (4).
(10) Gale, B. K.; Caldwell, K. D.; Frazier, A. B. *Anal. Chem.* **2001**, *73*, 2345−2352.
(11) Gale, B. K.; Caldwell, K. D.; Frazier, A. B. *IEEE Micro Electro Mech. Syst.* **1997**, 119−124.
(12) Gale, B. K.; Caldwell, K. D.; Frazier, A. B. *IEEE Trans. Biomed. Eng.* **1998**, *45*, 1459−1469.
(13) Gale, B. K.; Caldwell, K. D.; Frazier, A. B. *Anal. Chem.* **2002**, *74*, 1024−1030.

10.1021/ac0257647 CCC: $22.00
Published on Web 09/17/2002

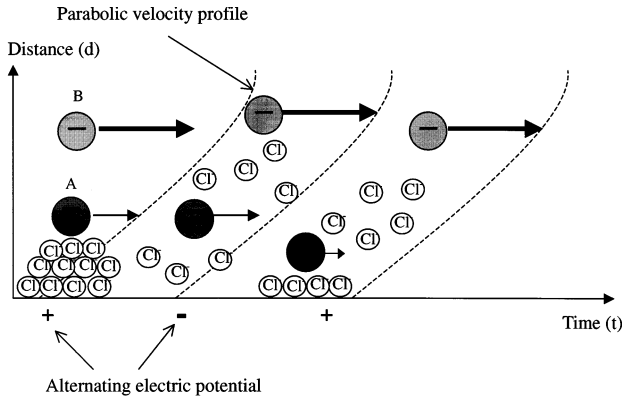

Figure 1. Schematic illustration of pulsed voltage EFFF. Depending on surface charge and size, the analyte components A and B are distributed in a distance *d* to the accumulation wall and travel with different velocities due to the parabolic flow profile.

A pulse reversing technique[14] widely used in electroplating industries would be applicable to reduce the polarization effect in μ-EFFF. In electroplating, a steady counterion layer is formed on the plating substrate when dc supply is used and obstructs other ions from reaching the substrate. In pulse reversal plating, the applied voltage is periodically reversed to cause this layer to discharge and allow easier passage of ions to the substrate.

In this study, a pulsed voltage (PV) μ-EFFF device fabricated in indium tin oxide (ITO)-coated glass is demonstrated. The current response and its corresponding electric field for constant and pulsed voltage were studied. The effect of pulse frequency on the retention time of latex particles was measured. By using PV, improved separation performance of latex particles with different particle size and surface charge was demonstrated.

THEORY

EFFF relies on an electric field perpendicular to the pressure-driven flow with parabolic velocity profile (Figure 1).[15] Electrically charged particles injected into the system are driven by the electric field toward the accumulation wall. Negatively charged particles accumulate on the wall adjacent to the positive electrode. Their accumulation creates a concentration gradient that causes particles to diffuse away from the wall. At equilibrium, the balancing of these opposing transport processes leads to a cloud of particles in a distance *d* to the accumulation wall. The migration force *F* toward the wall can be written as a product of the particle charge and the electric field. The strength of particle interaction with the electric field partitions the particles in a particular lamina of the parabolic flow profile with distance *d* from the accumulation wall. A strong interaction will force the particles closer to the accumulation wall while a weak interaction will distribute them more in the middle of the channel. Due to the parabolic flow profile of the pressure-driven flow, particles in the middle of the channel migrate faster than particles closer to the channel wall. Therefore, the retention time of particles depends on their interaction with the electric field. Particles having the weakest interaction will elute first followed by those with increasing interaction.

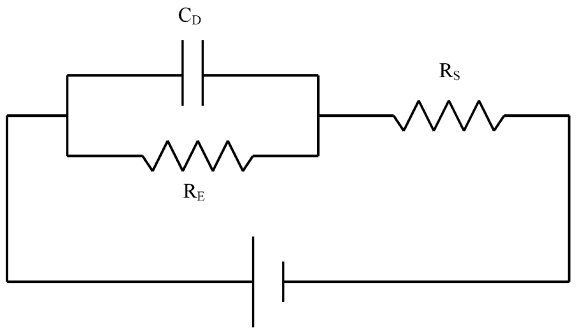

Figure 2. Equivalent circuit representation of a μ-EFFF device (R, resistor; C, capacitor).

Circuit Model. An equivalent circuit model[10,16] is postulated to explain the experimental observations in μ-EFFF separation. The equivalent circuit of the μ-EFFF device is composed of two serial RC elements and a serial resistor. The capacitance of the RC element corresponds to the double layer at the electrode−electrolyte interfaces, and the resistance corresponds to the charge-transfer resistance of electroactive species. The resistor serial to the two RC elements, R_S, represents the resistance of the electrolyte between the two electrodes. The two serial RC elements can be simplified to a single element resulting in the equivalent circuit for a μ-EFFF device depicted in Figure 2. If no electroactive species is present, the resistance of R_E will be very high. Therefore, when applying a constant voltage, charges will be built up in the capacitor and no current will flow via the highly resistive R_E route. The current will continue to flow as long as the double-layer capacitor C_D is not fully charged. Once the double layer reaches its full charge capacity, there will be a significant potential drop at the electrode−electrolyte interface and only very little current will flow through the RC element. In the μ-EFFF system, the strength of electric field is directly proportional to the drift current. Therefore, it is crucial to maintain a high current to ensure a significant electric field available in the channel for the separation. One possibility to address this problem is to decrease the resistance of R_E by adding electroactive species into the electrolyte (e.g., quinhydrone).[17] In our approach, we increase the current flowing across C_D by using a PV modulation.

The behavior of the current with time in a RC circuit at a constant voltage (CV) can be written as[18]

$$i = (V/R_S)e^{(-t/\tau)} \qquad (1)$$

where τ is the RC time constant, equal to R_SC_D, and V is the amplitude of the voltage.

As seen from eq 1, the current drops exponentially at the CV mode and the decaying rate largely depends on the time constant τ. By taking natural logarithm for both sides of eq 1, the equation

(14) Mridha, C. H.; Siew, S.; Sarkar, Y. K.; Chan, G. *Mater. Res. Soc. Symp.−Proc.* **2000**, *612*, D911−D917.
(15) Schimpf, M. E.; Caldwell, K.; Giddings, J. C. *Field flow fractionation handbook*; Wiley-Interscience: New York, 2000.
(16) Palkar, S. A.; Schure, M. R. *Anal. Chem.* **1997**, *69*, 3223−3229.
(17) Schimpf, M. E.; Russell, D. D.; Lewis, J. K. *J. Liq. Chromatogr.* **1994**, *17*, 3221−3238.
(18) Bard, A. J.; Faulkner, L. R. *Electrochemical methods: fundamentals and applications*, 2nd ed.; John Wiley: New York, 2001.

can be rewritten as

$$\ln i = (-1/\tau)t + \ln(V/R_S) \quad (2)$$

The RC time constant τ and electrolyte resistance R_S of the μ-EFFF system can be determined from the slope of the plot of ln i versus t and the y-intercept $\ln(V/R_S)$, respectively.

The current profile at the PV mode for a pulse duration of T can be expressed as

$$i = \begin{cases} \frac{V_{pos}}{R_S} e^{(-t/\tau)} & \text{for } t < T_{pos} \\ \frac{V_{neg}}{R_S} e^{(-t/\tau)} & \text{for } T_{pos} \le t \le T = T_{pos} + T_{neg} \end{cases} \quad (3)$$

where V_{pos} and V_{neg} are the voltage values at the positive and negative pulses, respectively, and T_{pos} and T_{neg} are their corresponding durations.

As seen in eq 2, the shorter the total pulse duration T, i.e., the reciprocal of the pulse frequency, the larger the remaining current.

In theory, the current increases with the increase of pulse frequency to enhance the electric field needed for the separation. Nonetheless, as will be seen in Results and Discussion, the improvement of particle separation/retention occurs at an intermediate pulse frequency at which the nanoparticles, influenced by the electric field, are allowed to equilibrate to specific locations in the flow channel. Higher frequency pulses will not improve the separation as the particles are not given sufficient time to respond.

EXPERIMENTAL METHODS

Materials. *Samples.* Native latex polystyrene (PS) particles and carboxylated surface-modified PS particles (hereafter termed as unmodified and modified particles, respectively) of 0.45- and 0.105-μm diameters with 3.8% and 4.6% standard deviation, respectively (Sigma Chemical, St. Louis, MO) or mixtures thereof were used as samples.

Carriers. The carrier solutions were either pure deionized water (Milli-Q system, Millpore, Bedford, MA) or solution containing 10 μM sodium chloride. Carrier solutions were filtered through a 0.44-μm filter and purged with nitrogen gas to remove the dissolved oxygen prior use.

μ-EFFF Device. The μ-EFFF device was fabricated in ITO-coated glass with a total thickness of 3 mm and an ITO sheet resistance of 12 Ω/□ (Samsung). A spacer made from Su-8 photoresist (Microchem) was used to define the μ-EFFF channel.

Device Fabrication. The μ-EFFF device was fabricated using a surface micromachining technique as outlined in Figure 3. The starting materials were two 10 × 10 cm^2 glass with one-sided ITO coating. ITO electrodes were first patterned using photolithography followed by wet etching in $HCl/HNO_3/H_2O$ with a volume ratio of 4:2:1 at room temperature (Figure 3a). Inlet and outlet ports with a diameter of 1.6 mm for external fluid connection were drilled in the upper glass plate (Figure 3b). The adhesion of the Su-8 photoresist on the ITO film was increased by an oxygen plasma treatment (50 °C for 3 min) of the ITO surface prior to spin-coating at 1250 rpm for 30 s. The sheet resistance of the ITO electrode increased to 14 Ω/□ after the oxygen plasma treatment. To eliminate thickness irregularities in the Su-8 layer, the substrate was placed level for 1 h before the soft bake was performed at 60 °C for 5 min followed by 90 °C for 3 min. A mask defining the channel geometry was aligned, and the substrate was exposed to UV light followed by a bake at 60 °C for 5 min, 90 °C for 3 min and photoresist development. The Su-8 photoresist channel is of ribbonlike structure with triangular ends (40 μm height, 10-mm breadth and 90-mm length). A closed channel of 40-μL volume was formed by bonding two substrates together (Figure 3c) in a hot pressing machine. The region between the substrates that was not making up the channel was filled with epoxy glue to stabilize the bonding. PEEK tubing with outer and inner diameters of 1.6 and 0.127 mm, respectively, was connected to the inlet and outlet of the device by using epoxy glue.

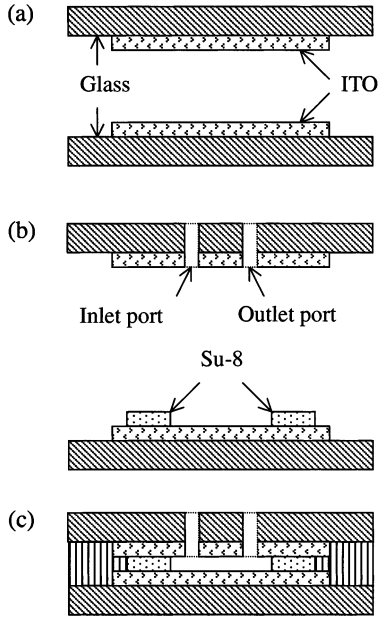

Figure 3. Fabrication of the μ-EFFF device. (a) Patterning of ITO electrodes on the top and bottom glasses. (b) Drilling inlet and outlet ports into the top glass. Channel creation on the bottom glass by photolithography with Su-8 photoresist. (c) Bonding the two glasses to complete the μ-EFFF device.

Instrumentation. A scheme of the μ-EFFF system setup is illustrated in Figure 4. The system comprises the μ-EFFF device, a potentiostat (PGSTAT30, Autolab, Eco Chemie B.V.), a digital syringe pump (SP200i, World Precision Instruments Inc.), a sample injection valve with sample loop (9250i, Rheodyne), a 1-μL syringe connected to the sample loop (Hamilton, Reno, NV), and a UV spectrophotometer equipped with a 1-μL flow cell (UVIS-201, Linear Instruments) at the outlet port. The UV spectrophotometer was connected to a personal computer via a data acquisition and AD/DA interface (NCI 900 interface system, PE Nelson, Perkin-Elmer, Shelton, CT). A Turbochrom software package (Perkin-Elmer) was used for data acquisition and analysis.

Methods. *Pulsed Voltage Scheme.* A rectangular PV waveform with alternating positive and negative polarity (V_{pos}, V_{neg}) of the same amplitude was applied across the two ITO electrodes to generate the electric field. The current response was studied for a pulse duty cycle δ, defined as $T_{pos}/(T_{pos} + T_{neg})$, of 0.5 at a voltage of 1.73 V and a frequency of 5 Hz. The effect of pulse frequency on particle retention was studied by the frequency modulation ranging from 2.5 to 62 Hz at a duty cycle of 0.5 and

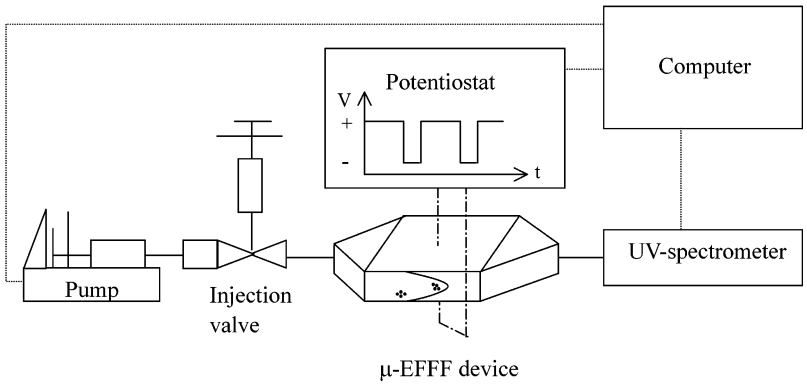

Figure 4. Schematic diagram of the experimental setup for μ-EFFF.

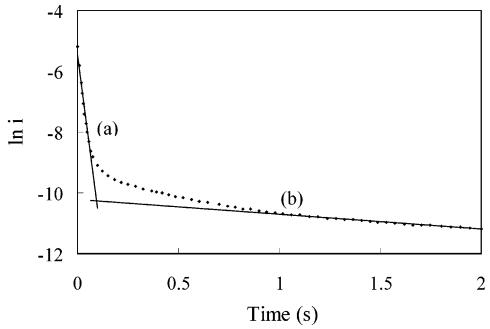

Figure 5. Logarithmic current as a function of time. The RC time constant is determined from the slop of the plot ln *i* versus *t* in region a. The current behavior in region b is caused by a "delayed buildup" of the double layer of which outer parts are sheared away by the carrier fluid flow.

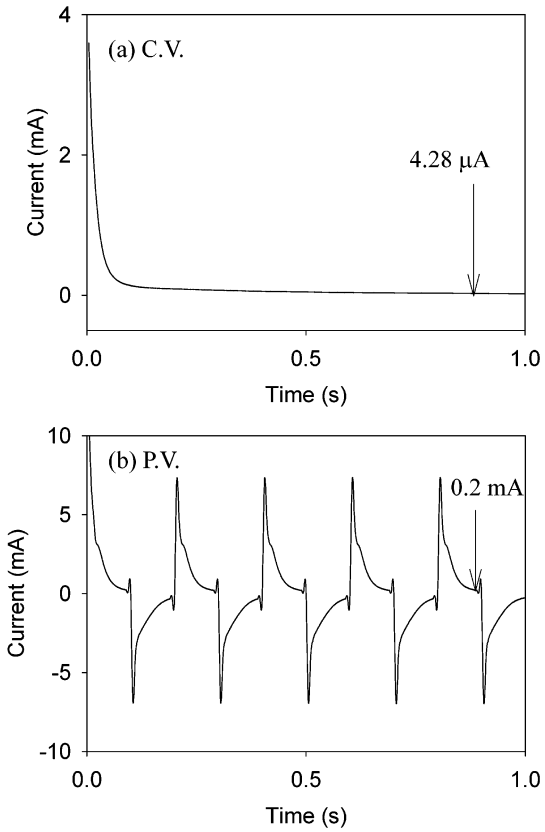

Figure 6. Current response as a function of pulse frequency. (a) Application of a CV of 1.73 V results in a current of 4.28 μA. (b) A higher current of 0.2 mA was observed at the same potential by applying a PV of 5 Hz.

at a voltage of 1.75 V. A 10 μM NaCl solution at a flow rate of 17 μL min^{-1} was used as carrier solution. Separation of particles with different surface charge was studied for a duty cycle of 0.9 at a voltage of 1.52 V and a frequency of 9 Hz. Separation of particles with different size was studied for a duty cycle of 0.8 at a voltage of 1.4 V and a frequency of 2.2 Hz. Deionized water was used as carrier solution at a flow rate of 17 μL min^{-1}.

Operation. One opening of the injection valve was connected to the PEEK tubing at the inlet port of the μ-EFFF device, and the other opening was connected to a digital syringe pump via PEEK tubing. A nanoparticle sample (0.05 wt %) of 0.3-μL volume was transported into the device by the carrier solution driven by the digital syringe pump. The pump flow was stopped after the sample plug entered the device, and a positive peak voltage was applied for 1 min followed by either a PV scheme or CV for 20 min for sample relaxation. Still applying the chosen voltage scheme, the syringe pump was restarted with a constant carrier flow of 17 μL min^{-1} to start the separation process. The electric current between the ITO electrodes as well as the UV adsorption (280 nm) caused by particles passing the flow cell was recorded with a personal computer.

RESULTS AND DISCUSSION

RC Time Constant. The carrier solution resistance and double-layer capacitance were characterized by a CV experiment. A voltage of 1.75 V was applied, and the current response was registered. R_S and C_D were calculated using eq 2. As shown in Figure 5, the behavior of current with time at the CV mode can be approximated by two linear functions labeled (a) and (b). Function a corresponds to the linearized eq 2 with the negative slope $1/\tau$ and the *y*-intercept ln(V/R_S). Function b corresponds to a "delayed buildup" of the double layer caused by the carrier fluid flow. Carrier solution resistance and double-layer capacitance were found to be 423 Ω and 46.9 μF, respectively. Theoretical carrier solution resistance was calculated as 493 Ω based on channel dimensions and the Na^+ and Cl^- equivalent ionic conductivities of 50.08×10^{-4} and 76.31×10^{-4} (m^2 S)/mol, respectively.[19] Experimental and theoretical values are of good consistency, indicating the applicability of the equivalent circuit model. A RC

(19) Lide, D. R. L., Ed. *CRC handbook of chemistry and physics*; CRC Press: Boca Raton, FL, 1996.

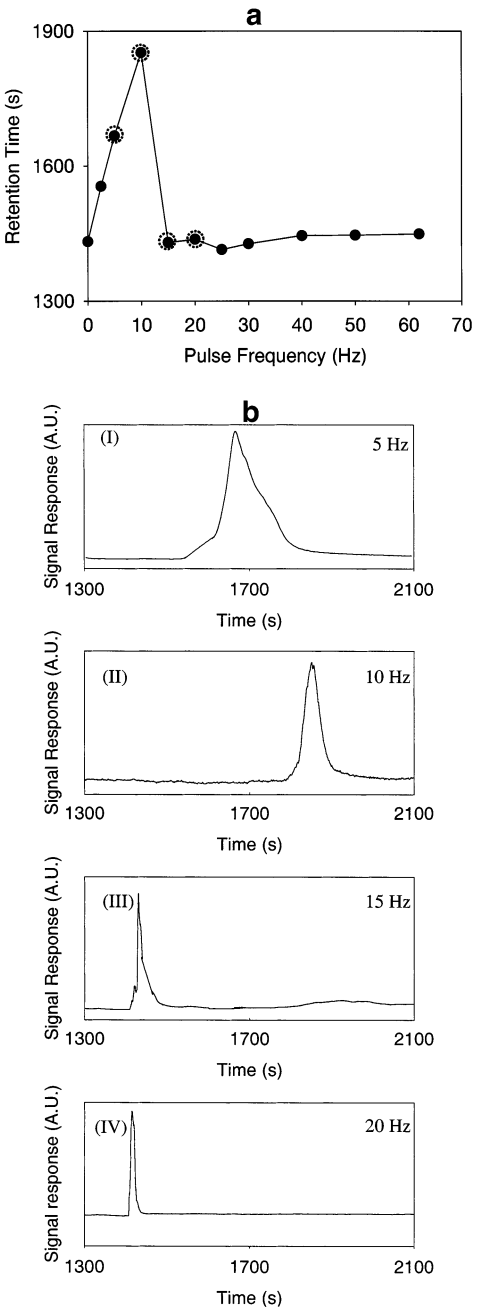

Figure 7. Retention time of modified PS particles as a function of the pulse frequency. The retention time increases with increasing pulse frequency to its maximum at 10 Hz and decreases to the same value observed for CV for higher frequencies (a). Retention profiles of particles at four frequencies (5, 10, 15, 20 Hz) are presented in (b I-IV), respectively (labeled with dotted circles in a).

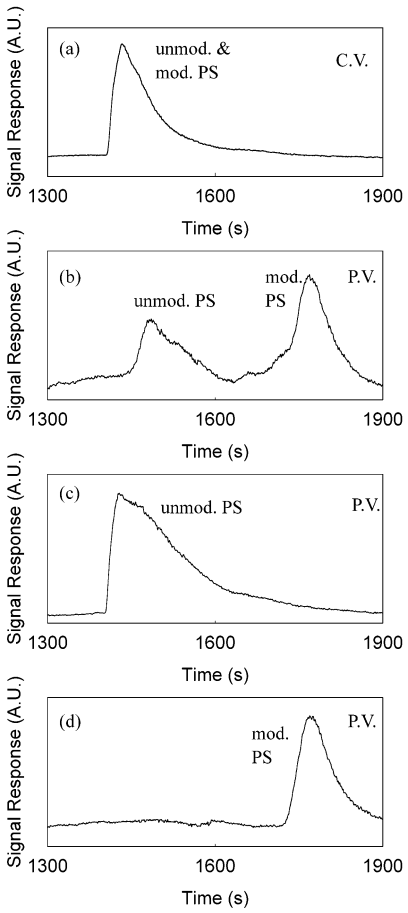

Figure 8. Fractionation of PS particles as a function of surface charge and frequency. (a) No separation was observed for mixtures of PS particles with and without surface modification using a CV (1.52 V). (b) Baseline separation was performed for the same particle mixture using a PV of 9 Hz with an amplitude of 1.52 V and a duty cycle of 0.9. (c, d). PS particles with higher surface charge (mod. PS) were identified to elute later than particles with lower surface charge (unmod. PS).

time constant of 0.020 s was calculated from the experimental results. This value is comparably smaller than RC time constants reported by other groups.[13,16] Therefore, because of a small time constant in our device, the current at the CV mode decays quickly (eq 1) and the PV operation is advantageous to increase the current of the device.

Current Response. Current flow is an indicator of the effective electric field in the channel. Current responses were registered after a CV or a PV was applied to the system. Figure 6a shows the current response as a function of time for a CV of 1.73 V. After the double-layer capacitor C_D was charged over the duration of 40 time constants, a residual current of ~4 μA was measured. In comparison, the current at the PV was found to be 50-fold higher and was measured as 0.2 mA (Figure 6b). This result can be explained by the shorter time given for current to decay exponentially as discussed in the theory section.

The effective electric field is directly proportional to current. A larger current at the PV mode gives a stronger effective field as compared to the CV mode. The ratio of effective to total voltage was found to be 0.12% for the CV mode and 5.7% for the PV mode.

Effect of Pulse Frequency. The retention time of PS particles (0.45 μm, modified) was studied as a function of the pulse frequency. Figure 7a shows that the retention time increases from 1400 s at the CV mode to 1800 s at 10 Hz. Further increase of the frequency resulted in a decrease of the retention time, and the retention time returns to the level of the CV mode. Exemplary particle retention profiles observed at the frequencies of interest (5, 10, 15, 20 Hz) are depicted in Figure 7b I-IV, respectively. In principle, a higher residual current is expected at higher frequencies, and thus, a stronger electric field results. However, when the pulse frequency is increased up to a point where there is no sufficient response time allowed for the particles to interact with

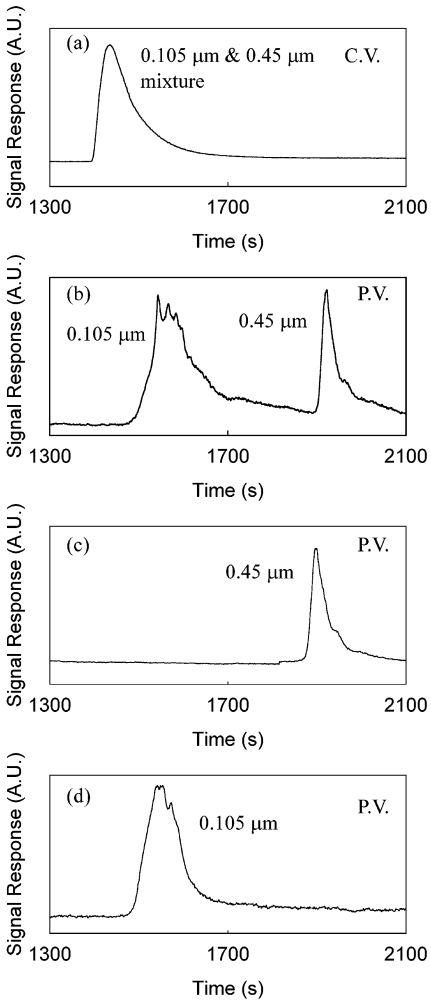

Figure 9. Fractionation of PS particles as a function of particle size and frequency. (a) No separation was observed for mixtures of PS particles with 0.105- and 0.45-μm diameter using a CV (1.4 V). (b) Separation was performed for the same mixture using a PV of 2.2 Hz with an amplitude of 1.4 V and a duty cycle of 0.8. (c, d). PS particles with larger diameter (0.45 μm) were identified to elute later than PS particles with 0.105-μm diameter.

the electric field, the retention time of particles decreases accordingly.

Separation Performance. *Particle Surface Charge.* The retention time of PS particles was studied as a function of their surface charge. Unmodified and carboxylate-modified PS particles (0.45 μm) corresponding to low and high surface charges, respectively, and mixtures thereof were separated by using CV and PV. Figure 8a reveals that no separation of particle mixtures was performed at CV. While under the same condition but applying a PV, two retention peaks were recorded at 1500 and 1800 s (Figure 8b), indicating the separation of the particle species. The peak at 1500 s (Figure 8c) was identified to originate from the unmodified PS and the peak at 1800 s (Figure 8d) from surface-modified PS particles. The increased retention time of surface-modified particles is in accordance with the theoretical expectation that they are of higher surface charges and interact stronger with the electric field.

Particle Size. The retention time of PS particles was studied as a function of their size. Particles of 0.45 and 0.105 μm in diameter and mixtures thereof were separated by using CV and PV. No separation of the particle mixture was registered at the CV mode (Figure 9a). In comparison, two retention peaks were recorded at 1550 and 1900 s by using the PV mode (Figure 9b). The retention peak at 1900 s (Figure 9c) was identified to originate from 0.45-μm particles and the peak at 1550 s from 0.105-μm particles (Figure 9d). The retention time was found to be proportional to the particle size. The dispersion seen in the first peak in Figure 9b and d may be caused by the nonuniform particle size of the sample.

CONCLUSION

An alternative approach in μ-EFFF to increase the effective electric field and to improve separation performance was demonstrated. A pulsed voltage with alternating polarity was applied on a microdevice having indium tin oxide electrodes. In comparison to constant voltage mode, a 50-fold higher current was observed, resulting in an increased effective electric field in the flow channel of the device. A strong influence of the pulse frequency on the retention time of nanoparticles was observed with a peak maximum at 10 Hz. Particle mixtures of different surface charge or particle size were successfully separated. Further studies will be conducted to develop a detailed theory on pulsed voltage separation. We believe that our approach enables improved adaptation to sample requirements by modulating the pulse frequency, duty cycle, potential, and waveform. In particular, pulsed voltage μ-EFFF can be potentially developed to be a tool for biological sample pretreatment in μ-TAS systems.

ACKNOWLEDGMENT

This work was supported by grants from the Innovation & Technology Commission of the Hong Kong SAR (AF/150/99) and the Hong Kong Jockey Club. The authors also thank the Biotechnology Research Institute at HKUST for providing the laboratory facility for this work.

Received for review May 11, 2002. Accepted August 25, 2002.

AC0257647